HAL
open science

Mass transfer into a spherical bubble

A. Saboni, Silvia Alexandrova, M. Karsheva, Christophe Gourdon

To cite this version:

A. Saboni, Silvia Alexandrova, M. Karsheva, Christophe Gourdon. Mass transfer into a spherical bubble. Chemical Engineering Science, 2016, 152, pp.109-115. 10.1016/j.ces.2016.06.001 . hal-01905213

HAL Id: hal-01905213

https://hal.science/hal-01905213

Submitted on 25 Oct 2018

HAL is a multi-disciplinary open access archive for the deposit and dissemination of scientific research documents, whether they are published or not. The documents may come from teaching and research institutions in France or abroad, or from public or private research centers.

L'archive ouverte pluridisciplinaire **HAL**, est destinée au dépôt et à la diffusion de documents scientifiques de niveau recherche, publiés ou non, émanant des établissements d'enseignement et de recherche français ou étrangers, des laboratoires publics ou privés.

Open Archive Toulouse Archive Ouverte

OATAO is an open access repository that collects the work of Toulouse researchers and makes it freely available over the web where possible

This is an author's version published in: http://oatao.univ-toulouse.fr/20504

To cite this version:

Saboni, Abdellah and Alexandrova, S. and Karsheva, M. and Gourdon, Christophe *Mass transfer into a spherical bubble.* (2016) Chemical Engineering Science, 152. 109-115. ISSN 0009-2509

Any correspondence concerning this service should be sent to the repository administrator: tech-oatao@listes-diff.inp-toulouse.fr

Short Communication

Mass transfer into a spherical bubble

A. Saboni [a], S. Alexandrova [b,*], M. Karsheva [c], C. Gourdon [d]

[a] Laboratoire SIAME-IUT, UPPA, Avenue de l'Université, 64 000 Pau, France
[b] Laboratoire de Thermique, Energétique et Procédés, ENSGTI-UPPA, Rue Jules Ferry, BP 7511, 64 075 Pau Cedex, France
[c] Department of Chemical Engineering, University of Chemical Technology and Metallurgy, Kl. Ohridski Blvd, 1756 Sofia, Bulgaria
[d] Laboratoire de Génie Chimique, ENSIACET, BP 1301, 4, allée Emile Monso, 31432 Toulouse, France

HIGHLIGHTS

- We model the hydrodynamics and mass transfer into a bubble.
- The effect of the Schmidt and of the internal Reynolds numbers on mass transfer is investigated.
- A predictive equation for the Sherwood number in terms of Schmidt and Reynolds numbers is derived.

ABSTRACT

A numerical study has been conducted to investigate the mass transfer inside a spherical bubble at low to moderate Reynolds numbers. The Navier–Stokes and diffusion–convection equations were solved numerically by a finite difference method. The effect of the bubble Schmidt number (over the range $0.1 < Sc_d < 5$) and of the internal Reynolds number (over the range $0.1 < Re_d < 13$) on mass transfer is investigated. The results show that the mass transfer is strongly dependent on the Reynolds number and the Schmidt number. From the numerical results, a predictive equation for the Sherwood number in terms of the Schmidt number and the Reynolds number is derived.

1. Introduction

The understanding of heat or mass transfer in moving bubbles or drops is important for different physical problems dealing with waste water treatment, distillation, bubble column reactors, solvent extraction, sedimentation of particles, spraying and so on. Various researchers investigated analytically or numerically flow and heat or mass transfer from a bubble (Clift et al., 1978; Sadhal et al., 1996; Chhabra, 2006; Dani et al., 2006; Takemura and Yabe, 1998; Saboni et al., 2007; Juncu, 1999; Legendre and Magnaudet, 1999; Lochiel and Calderbank, 1964) at low to moderate Reynolds numbers. A large amount of studies have considered mass transfer into bubbles or drops at creeping flow (Clift et al., 1978; Sadhal et al., 1996; Chhabra, 2006; Johns and Beckmann, 1966; Watada et al., 1970; Oliver and Chung, 1986; Juncu, 2001) but less attention has been paid to the mass transfer into bubbles at moderate Reynolds numbers (Oliver and Chung, 1986; Juncu, 2001; Oliver and De Witt, 1995; Colombet et al., 2013; Juncu, 2010). By assuming molecular diffusion and neglecting the continuous phase resistance, Newman (1931) developed an analytical solution valid for stagnant spherical bubbles or drops ($Pe=0$). The instantaneous Sherwood number is given as

$$Sh = \frac{2\pi^2}{3}\frac{\sum_{n=1}^{+\infty}\exp\left(-[n\pi]^2\tau\right)}{\sum_{n=1}^{+\infty}\frac{1}{n^2}\exp\left(-[n\pi]^2\tau\right)} \tag{1}$$

where τ is the dimensionless time $\tau = Dt/a^2$ where D is the diffusivity, a is the bubble radius and t is time.

For a fluid sphere in a creeping flow ($Re \to 0$) with $Pe \to \infty$, Kronig and Brink (1950) assumed that the concentration/temperature during the heat/mass transfer was constant, along a given streamline at a given time. Using the Hadamard–Rybczynski (Hadamard, 1911; Rybczynski, 1911) solution for the fluid flow field, they developed an asymptotic expansion for the energy equation. Two new coordinates were chosen to solve the conduction–convection equation: a coordinate coinciding with the Stokes flow streamlines and a coordinate perpendicular to these streamlines.

With the new coordinate, Kronig and Brink (1950) obtained an analytical solution:

$$Sh = \frac{32}{3}\frac{\sum_{n=1}^{+\infty} A_n^2 \lambda_n \exp(-16\lambda_n \tau)}{\sum_{n=1}^{+\infty} A_n^2 \exp(-16\lambda_n \tau)} \tag{2}$$

where the coefficients A_n and λ_n are given in (Colombet et al., 2013; Lochiel and Calderbank, 1964).

For the case of intermediate Peclet number values, numerical solutions were obtained by Johns and Beckmann (1966) and Watada et al. (1970), who used the flow fields described by the Hadamard and Rybczinski analytical solutions. At higher Reynolds numbers numerical solutions of the Navier–Stokes and diffusion–convection equations have been obtained by many authors (Chen, 2001; Feng and Michaelides, 2001; Saboni et al., 2010, 2011). The numerical results show that the flows inside and outside the sphere significantly influence the mass transfer. Most of these investigations were in fact motivated by an interest on mass transfer into drops rather than mass transfer into bubbles. Few studies have been devoted to mass transfer into bubbles at moderate and large Reynolds numbers (Oliver and De Witt, 1995; Colombet et al., 2013; Juncu, 2010; Zaritzky and Calvelo, 1979). For instance, Juncu (2010) gives a detailed analysis of the numerical solving of the unsteady heat/mass transfer inside a circulating sphere in a creeping flow and in moderate Re numbers flows. The influence of the Pe and Re numbers on the heat/mass transfer rate was investigated for three fluid–fluid systems (gas bubbles in liquids, liquid drops in another immiscible liquid and liquid drops in gases). The results obtained for the liquid–liquid and liquid in gases systems are useful in practice. On the contrary, the results for the bubbles in a liquid at large Peclet number, should be used with caution. Indeed, a fluid sphere with a Reynolds number equal to one and a Peclet number equal to ten thousand requires a Schmidt number equal to ten thousand ($Pe_d = Re_d{}^*Sc_d$). Such large Schmidt number, is valid for the liquid phase but not for the gas phase where the Schmidt numbers are considerably smaller. It seems from the studies (Oliver and De Witt, 1995; Colombet et al., 2013; Juncu, 2010) that the Sherwood number may exceed the Kronig–Brink asymptotic value for internal Reynolds numbers greater than ten.

This study aims to complement earlier studies (Oliver and De Witt, 1995; Colombet et al., 2013; Juncu, 2010) and to check some statements focusing on the physical properties encountered in practice. In the present study, the mass transfer model from a continuous phase to a spherical bubble was developed. Firstly, we solve the Navier–Stokes equations, and obtain the flow fields inside and outside a spherical bubble. Then we use the velocity components for solving the diffusion–convection equation and derive the rate of mass transfer into a spherical bubble.

In previous studies (Oliver and De Witt, 1995; Colombet et al., 2013; Juncu, 2010) the results were analyzed on the basis of the evolution of Sherwood numbers only, here the results are analyzed in terms of streamlines inside and outside the spherical bubble, in terms of concentrations' contour maps inside the bubble, and in terms of variations in the average Sherwood number. This analysis helps to understand the mechanisms of mass transfer between the bubble and the continuous medium. Based on our numerical results a predictive equation for the asymptotic Sherwood number is proposed for the internal Reynolds number in the range $0.1 < Re_d < 13$ and Schmidt number from 0.1 to 5.

2. Governing equations

A clean bubble of radius a is considered. It is moving with uniform velocity U_∞ in another immiscible fluid of infinite extent volume. Since the flow is considered axisymmetric, the Navier–Stokes equations can be written in terms of stream function and vorticity (ψ and ω) in spherical coordinates r and θ:

$$E^2\psi_d = \omega_d r \sin\theta \tag{3}$$

and

$$\frac{Re_d}{2}\left[\frac{\partial\psi_d}{\partial r}\frac{\partial}{\partial\theta}\left(\frac{\omega_d}{r\sin\theta}\right) - \frac{\partial\psi_d}{\partial\theta}\frac{\partial}{\partial r}\left(\frac{\omega_d}{r\sin\theta}\right)\right]\sin\theta = E^2(\omega_d r\sin\theta) \tag{4}$$

where $E^2 = \frac{\partial^2}{\partial r^2} + \frac{\sin\theta}{r^2}\frac{\partial}{\partial\theta}\left(\frac{1}{\sin\theta}\frac{\partial}{\partial\theta}\right)$

Outside the bubble, the above equations are still valid, but for numerical reasons the radial coordinate r is transformed via $r = e^z$, where z is the logarithmic radial coordinate. The results are as follows:

$$E^2\psi_c = \omega_c e^z \sin\theta \tag{5}$$

and

$$\frac{Re_c}{2}\left[\frac{\partial\psi_c}{\partial z}\frac{\partial}{\partial\theta}\left(\frac{\omega_c}{e^z\sin\theta}\right) - \frac{\partial\psi_c}{\partial\theta}\frac{\partial}{\partial z}\left(\frac{\omega_c}{e^z\sin\theta}\right)\right]e^z\sin\theta = e^{2z}E^2(\omega_c e^z\sin\theta) \tag{6}$$

All variables are normalized by introducing the following dimensionless quantities:

$$r = r'/a;\ \ \omega = \omega' a/U\infty;\ \psi = \psi'/(U\infty\, a^2);\ \ Re_d = 2\,a\,U\infty/\nu_d;$$
$$Re_c = 2\,a\,U\infty/\nu_c$$

where the primes denote the dimensional quantities and subscripts d and c refer to dispersed and continuous phase, respectively, a is the bubble radius, U_∞ is the terminal velocity, ν is the kinematic viscosity, Re_d is the Reynolds number based on dispersed phase properties and Re_c is the Reynolds number based on continuous phase properties. The relation between Reynolds numbers, is given by $Re_d = Re_c\frac{\rho_d\mu_c}{\rho_c\mu_d}$. For an air bubble in water, with $\mu_d/\mu_c = 1/55$ and $\rho_d/\rho_c = 1/836$, the relation between the two Reynolds numbers is $Re_d = Re_c/15.2$.

In terms of dimensionless stream function ψ, the dimensionless radial and tangential velocities are given by:

$$u = -\frac{1}{r^2\sin\theta}\frac{\partial\psi}{\partial\theta};\qquad v = \frac{1}{r\sin\theta}\frac{\partial\psi}{\partial r} \tag{7}$$

The boundary conditions to be satisfied are:

i) Far from the bubble ($z = z\infty$), undisturbed parallel flow is assumed: $\omega_c = 0$; $\psi_c = 0.5e^{2z}\sin^2\theta$.
ii) Along the axis of symmetry ($\theta = 0, \pi$): $\psi_c = 0$, $\omega_c = 0$, $\psi_d = 0$, $\omega_d = 0$.
iii) Across the interface ($z = 0$ *or* $r = 1$), the following relations account for, respectively: negligible mass transfer, continuity of tangential velocity, continuity of tangential stress (no surface tension variation):

$$\psi_c = 0 \text{ and } \psi_d = 0;\ \ \frac{\partial\psi_c}{\partial z} = \frac{\partial\psi_d}{\partial r};\ \ \frac{\mu_c}{\mu_d}\left(\frac{\partial^2\psi_c}{\partial z^2} - 3\frac{\partial\psi_c}{\partial z}\right) = \left(\frac{\partial^2\psi_d}{\partial r^2} - 2\frac{\partial\psi_d}{\partial r}\right)$$

where μ is the dynamic viscosity.

Eqs. (3)–(6) subjected to the boundary conditions (i)–(iii) are solved simultaneously to obtain stream-function and vorticity values. Once stream function is known, the velocities can be determined from Eq. (7). The concentration distribution can then be calculated from the diffusion–convection equation. Since the flow is considered axisymmetric, the unsteady convective mass transfer into a bubble in spherical coordinates r and θ is described by the following dimensionless diffusion convection equation:

$$\frac{\partial C}{\partial\tau} + \frac{Pe}{2}\left(u\frac{\partial C}{\partial r} + \frac{v}{r}\frac{\partial C}{\partial\theta}\right) = \frac{\partial^2 C}{\partial r^2} + \frac{2}{r}\frac{\partial C}{\partial r} + \frac{1}{r^2}\left(\frac{\partial^2 C}{\partial\theta^2} + \cot(\theta)\frac{\partial C}{\partial\theta}\right) \tag{8}$$

where Pe is the Peclet number $(Pe = 2aU_\infty/D)$, a is the bubble radius, and C is the dimensionless concentration $C = C'/C_i'$ where C_i' is the concentration at the interface.

The boundary and initial conditions to be satisfied are:

i) Initial condition: $C(r, \theta, t = 0) = 0$.

ii) Along the axis of symmetry: $\left.\frac{\partial C}{\partial \theta}\right|_{\theta=0} = \left.\frac{\partial C}{\partial \theta}\right|_{\theta=\pi} = 0$.

iii) Across the interface: $C(r = 1, \theta, t) = 1$.

The surface and average Sherwood numbers are computed from the mass transfer flux from the bubble surface:

$$Sh_{surface} = -\frac{2}{\overline{C}}\left(\frac{\partial C}{\partial r}\right)\Big|_{r=1} \tag{9}$$

$$Sh = -\frac{1}{\overline{C}}\int_0^\pi \left(\frac{\partial C}{\partial r}\right)\Big|_{r=1} \sin\theta \, d\theta \tag{10}$$

The average concentration is computed from the following equation:

$$\overline{C} = \frac{3}{2}\int_0^1 \int_0^\pi C(r, \theta, \tau) r^2 \sin\theta d\theta dr \tag{11}$$

3. Numerical method

We solve the partial differential equations that describe the motion inside and outside the bubble and the concentration inside the bubble, as given by Eqs. (1)–(8), together with the above boundary conditions evaluated numerically by finite difference approximations. The elliptic stream function equations are solved iteratively, the parabolic vorticity equations are solved by means of the Alternating Direction Implicit method. Once stream function is known, the velocities are then determined from Eq. (7). The convection–diffusion equation is solved by means of the Alternating-Direction Explicit (ADE) scheme (Barakat and Clark, 1966). Numerical experiments were performed in order to check the grid independence of the solutions and grid size of 181 × 181 elements in the dispersed phase and 401 × 181 in the continuous phase (N_r =181, N_θ=181 and N_z=401) was adopted for grid-free solution throughout the calculations in the present study. The distance from the bubble to the edge of the computational domain is 100 diameters for small Reynolds numbers and 12 diameters for higher Reynolds numbers for which the boundary layer thickness is less. The validation of the numerical methods used implied two stages: (1) the checking of the numerical solution procedure concerning the hydrodynamics around and inside a bubble, and (2) the checking of the numerical method used for the mass transfer. Detailed discussions on the accuracy of the solution procedure employed for the momentum, continuity equations, and diffusion–convection equation were made elsewhere (Feng and Michaelides, 2001; Saboni et al., 2010).

Before presenting new results on mass transfer into a spherical bubble, it is essential to validate the present computer code. As noted earlier, since extensive validation of the numerical method used here, for a variety of cases such as clean or contaminated fluid spheres have been reported elsewhere (Saboni et al., 2010, 2011) only few additional validations for hydrodynamics and mass transfer into bubbles are presented here. The numerical solution procedure used in this work has been validated by comparing the present results with those from the literature. Concerning the hydrodynamics part, we validate the numerical scheme against the results of Legendre (2007) who simulated the flow around the bubble. A correlation based on the best fitting of these numerical results was proposed to estimate dimensionless maximal velocity, U_{max}/U_∞ at bubble interface as a function of the Reynolds number (Legendre, 2007):

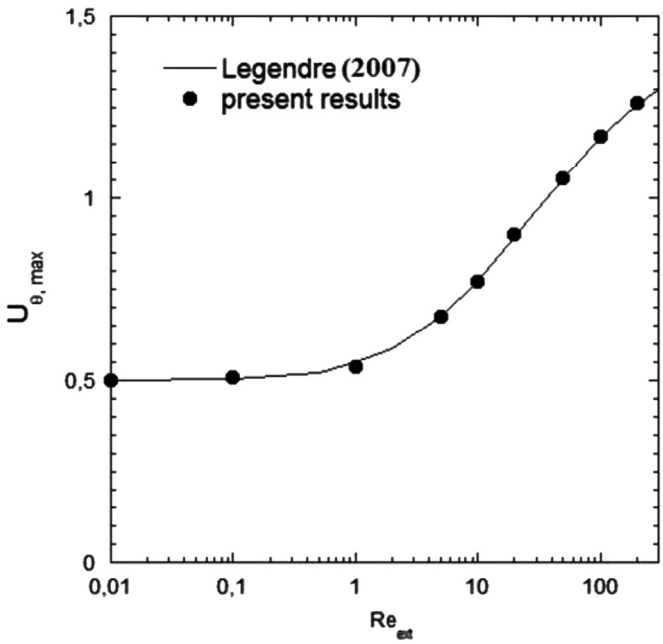

Fig. 1. Maximum velocity at the bubble interface versus external Reynolds number of a bubble.

$$U_{max} = \frac{1}{2}\frac{16 + 3.315\sqrt{Re_c} + 3\,Re_c}{16 + 3.315\sqrt{Re_c} + Re_c}U_\infty \tag{12}$$

Values of maximal velocity, U_{max}/U_∞ at bubble interface from the Eq. (12) are presented in Fig. 1 and compared to those from our numerical results. From Fig. 1, it is evident that for all Reynolds numbers it exists an excellent agreement between our results and those of Legendre correlation (Legendre, 2007). It should be noted that the good agreement between our results, which are derived from a coupling between the flow inside the bubble and the flow outside of the bubble and those of Legendre (2007) based on the simulation of the external flow only validates the hypothesis that considers the surface of the bubble as shear free interface. This hypothesis coupled to the solution of the Navier–Stokes equations outside the bubble, allows to obtain the velocity fields and drag coefficients without necessity to know the details of the flow inside the bubble. The knowledge of the flow within the bubble is necessary if one is interested in mass transfer inside it.

We present our numerical results focusing on the physical properties encountered in practice. The Peclet number is defined as $Pe_d = Re_d{}^*Sc_d$. At a temperature of 20 °C, the Schmidt number, the ratio (ν/D), is about 1 for gases but it is greater for lower temperatures. To account for the effect of temperature, the numerical computations have been carried out for Schmidt numbers ranging from 0.1 to 5. We consider continuous Reynolds numbers not exceeding 200 which is the highest limit for which the flow rests axisymmetric and for which an air bubble in water remains quasi-spherical. Viewed the Schmidt and Reynolds numbers considered, the results are valid for Peclet numbers less than 65 $(Pe_d \leq 65)$.

Concerning the mass transfer part, we validate the numerical scheme against the results of Juncu (2010). The asymptotic Sherwood numbers for a spherical bubble with different Schmidt number values are compared with those of Juncu (2010) in Table 1, which shows a good agreement between our results and those

Table 1
Comparison of the present results for the asymptotic Sherwood values with those from the numerical study of Juncu (2010).

Sc	$Re_d=1$		$Re_d=10$	
	Juncu (2010)	**Present results**	Juncu (2010)	**Present results**
0.1	–	6.58	6.59	6.59
0.5	–	6.58	6.93	6.96
1.0	6.58	6.58	7.88	8.00
1.5	–	–	–	9.38
2.0	–	6.60	10.51	10.77
2.5	–	–	–	12.00
3.0	–	6.64	–	13.01
3.5	–	–	–	13.83
4.0	–	6.69	–	14.48
4.5	–			14.99
5.0	6.74	6.76	15.32	15.39

from the previous study cited above. Other numerical simulations with much larger Peclet numbers (Pe_d from 100 to 10^5) were conducted and the obtained numerical results are in good agreement with those of Juncu (2010) which confirms the reliability of the computer code developed by Juncu (2010). However, these results do not correspond to a physical reality and are not presented here to avoid any misinterpretation or confusion.

4. Results and discussion

Fig. 2 shows streamline contours inside and outside a bubble for different dispersed Reynolds numbers $Re_d=0.1$, 1, 5, 10 and 13 corresponding respectively to continuous Reynolds numbers $Re_c=1.52$, 15.2, 76, 152 and 197.6. For all Reynolds numbers, the contour line plots show no flow separation downstream the bubble. Slight asymmetry is observed between upstream and downstream regions near the bubble. The internal flow departs from symmetry due to the effect of the external flow.

The isoconcentrations' contours inside a bubble for different dispersed Reynolds numbers ($Re_d=1$, 5 and 10) and a fixed Schmidt number ($Sc_d=3$) at time $\tau=0.1$, are plotted in Fig. 3. For $Re_d=1$, the shape of the isoconcentrations' contours is almost spherical and the average concentration is 0.77 which corresponds to the value given by the Newnan equation at time $\tau=0.1$. This means that transport by convection is very limited and the mass transfer occurs mainly by diffusion. For the case $Re_d=10$, the part of the convective transport increases, and the isoconcentrations' contours inside the bubble become deformed under the influence of the internal flow.

Fig. 4 shows the development in time of the concentration profiles inside the bubble. For short times, the radial concentration gradients near the surface of the sphere are very high, and mass is transferred mainly by diffusion similar to a stagnant bubble which absorbs solute in a radially symmetric shape. With the time, the convective effects prevail and the internal circulation brings the solute to the rear of the bubble. At large times, the concentration profiles inside the bubble become deformed under the influence of internal circulation. It is to be noted that the concentration profiles within the bubble fail to follow the streamlines since the Peclet number is not large enough for the convective transport to be completely dominant.

Fig. 5 shows the time history of the average Sherwood number for fixed Reynolds number $Re_d=1$ ($Re_c=15.2$) and a fixed Sc_d number ($Sc_d=5$). The figure shows that, initially, the Sherwood number is completely large because of strong concentrations' gradients between the surface and the interior of the bubble. The Sherwood number decreases with the time approaching an asymptotic value. At any time, numerical results coincide with the Newman analytical solution which implies that for low Reynolds numbers with Schmidt numbers between 0 and 5, the mass transfer occurs only by diffusion.

The time history of the average Sherwood number for fixed Reynolds number $Re_d=13$ ($Re_c=197.6$) and different Schmidt numbers ($Sc_d=0.5$–5.0) is shown on Fig. 6. At the beginning, the transfer is due mainly to diffusion but rather quickly the convection becomes the governing mechanism. Combination of both diffusion and convection allows the solute to be taken away from the interface. The Sherwood number decreases with time and approaches an asymptotic value increasing with the Schmidt number. For high Schmidt number it is observed that the instantaneous Sherwood number oscillates with decreasing amplitude. These oscillations which were also observed under creeping-flow conditions (Clift et al., 1978; Rybczynski, 1911) are due to the circulation inside the bubble.

In order to predict heat or mass transfer into drops or bubbles for moderate Reynolds numbers using results for small Reynolds

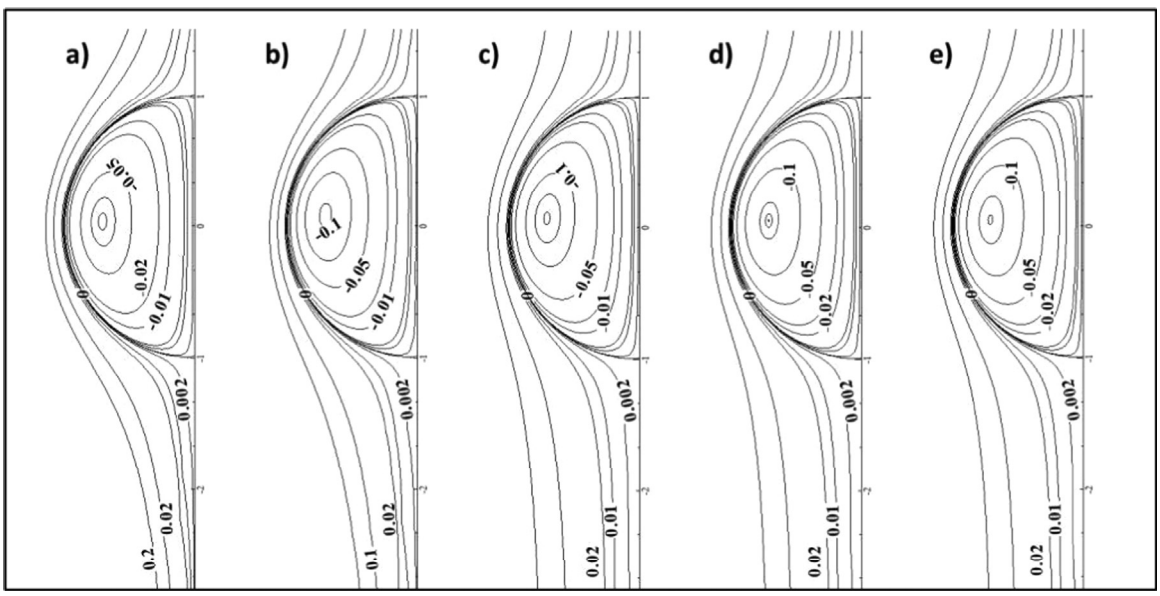

Fig. 2. Stream function contours, inside and outside a bubble for different Reynolds numbers (a) $Re_d=0.1$, (b) $Re_d=1$, (c) $Re_d=5$, (d) $Re_d=10$, (e) $Re_d=13$.

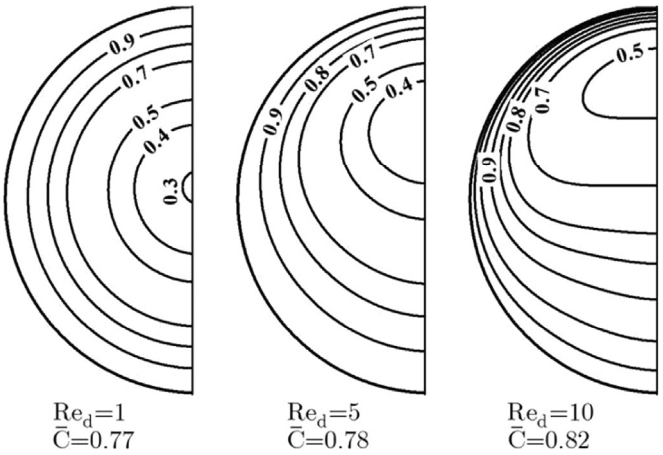

Fig. 3. Concentration contour lines inside a bubble for different Reynolds numbers and $Sc=3$ at time $\tau=0.1$.

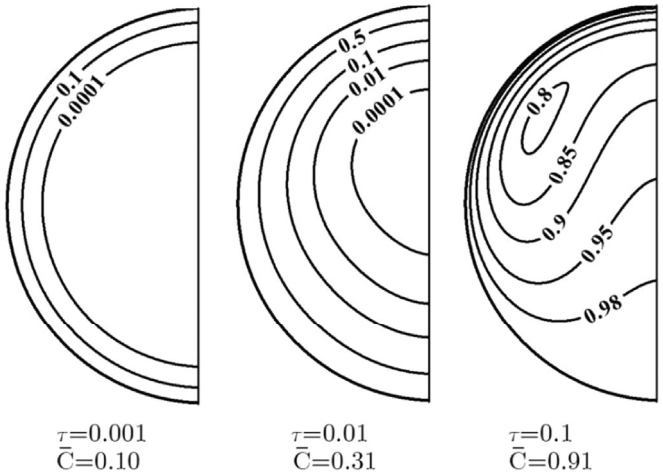

Fig. 4. Concentration contour lines inside a bubble as function of time for $Re_d=13$ and $Sc=5$.

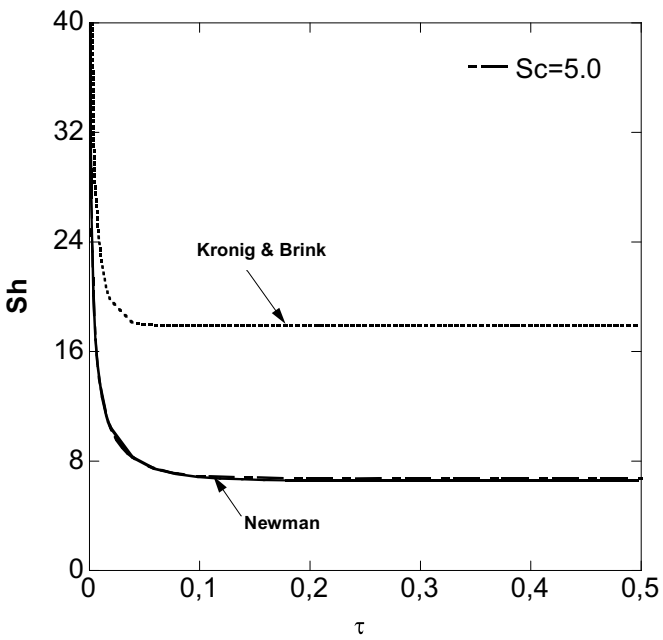

Fig. 5. Time variation of Sherwood number at $Re_d=1$ ($Re_c=15.2$).

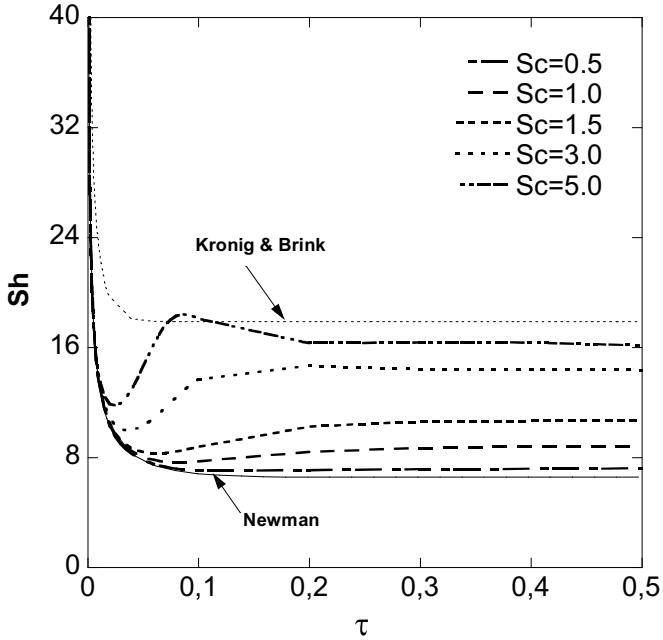

Fig. 6. Time variation of Sherwood number for different Schmidt number at $Re_d=13$ ($Re_c=197.6$).

numbers, Oliver and De Witt (1995) introduced an effective Peclet number. Juncu (2010) notes the validity of the effective Peclet number concept for $Pe_{eff}<200$ on behalf of two systems: liquid drops in other immiscible liquid and liquid drops in a surrounding gas. In the case of bubbles, the Oliver and De Witt (1995) effective Peclet number is reduced to the following expression:

$$Pe_{eff} = \left(1 + 0.4\ \log(0.3\ Re_c + 1)\right)Pe \tag{13}$$

Fig. 7 shows the evolution of our numerical asymptotic Sherwood number against the effective Peclet number. The numerical results show that the asymptotic Sh for different values of Re_d and Pe_{eff} are located on the same curve but deviate from the Clift et al. (1978) results. This coincides with the findings of Colombet et al. (2013) and confirms that the Oliver and De Witt (1995) effective Peclet number concept is not suitable for bubbles.

Table 2 summarizes the asymptotic average Sherwood number (Sh), obtained from our calculations for the range of parameters covered $Re_d=0.1$–13 ($Re_c=1.52$–197), and different Schmidt numbers ($Sc_d=0.1$–5). This table shows the influence of Re_d and Sc_d on the mass transfer. As expected, the Sherwood number increases with increasing the Schmidt number for fixed Reynolds numbers. For a fixed Reynolds number, the Sherwood number increases with the Schmidt number increase. The influence of the Schmidt number on the mass transfer is more or less important; depending on the Reynolds numbers. From Table 2 it appears, however, that the relative difference between the Sherwood values for $Sc_d=0.1$, $Sc_d=5$ is less than 3% for $Re_d<1$. On the contrary, for $Re_d=13$, the relative difference can be quite large, approaching 60%. This table also shows that the asymptotic values of the analytical solution of Kronig–Brink are never exceeded for spherical bubbles with Reynolds numbers $Re_d<13$ and Schmidt numbers $Sc_d<5$.

To present the numerical results in a more convenient form we tried to correlate our numerical results. A correlation of these numerical which is reduced to the Newman solution for $Re_dSc_d\to 0$, is as follows:

$$Sh = 6.57 + \left(\frac{Re_{\ d}Sc_d}{8.35 + 0.0125\left(Re_dSc_d\right)^{1.66}}\right)^2 \tag{14}$$

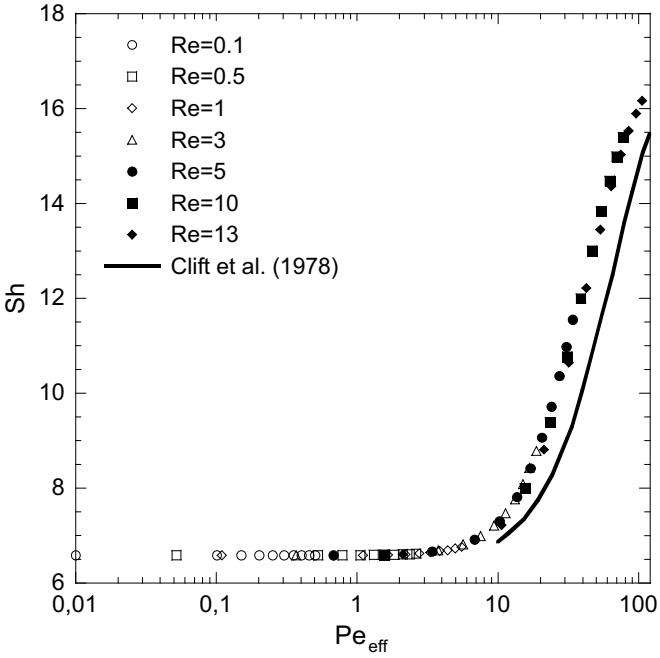

Fig. 7. Asymptotic values of average Sh number as a function of the effective Peclet number.

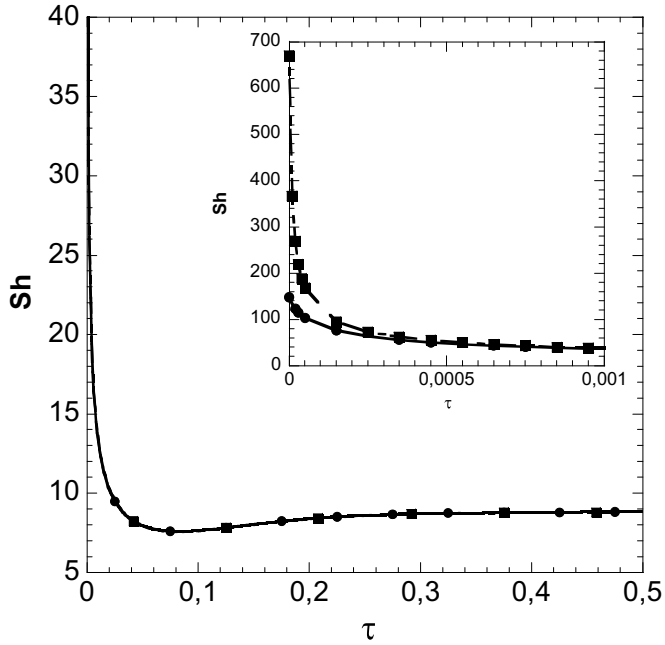

Fig. 8. Time variation of Sherwood number for $Sc=1$ and $Re_d=13$ ($Re_c=197.6$): (■) Steady flow, (●) transient flow.

Table 2
Asymptotic Sherwood values for different Schmidt and Reynolds numbers.

Sc	Re_d							
	0.1	**0.5**	**1**	**2**	**3**	**5**	**10**	**13**
0.1	6.58	6.58	6.58	6.58	6.58	6.58	6.59	6.60
0.5	6.58	6.58	6.58	6.58	6.60	6.66	6.96	7.22
1.0	6.58	6.58	6.58	6.61	6.68	6.91	8.00	8.81
1.5	6.58	6.58	6.59	6.65	6.81	7.30	9.38	10.64
2.0	6.58	6.58	6.60	6.71	6.99	7.81	10.77	12.22
2.5	6.58	6.59	6.62	6.79	7.21	8.41	12.00	13.44
3.0	6.58	6.59	6.64	6.88	7.47	9.06	13.01	14.36
3.5	6.58	6.59	6.67	6.99	7.76	9.72	13.83	15.03
4.0	6.58	6.60	6.69	7.12	8.08	10.36	14.48	15.53
4.5	6.58	6.60	6.73	7.25	8.43	10.98	14.99	15.89
5.0	6.58	6.61	6.76	7.40	8.78	11.55	15.39	16.16

The Sherwood number values derived by this formula coincide with those calculated numerically with an error less than 5% for bubbles with $0.1 < Re_d < 13$ and $0.1 < Sc_d < 5$.

5. A note on the steady state flow assumption

In this study as well as those of Clift et al. (1978), Oliver and De Witt (1995), Juncu (2010) and Colombet et al. (2013), the flow is assumed to be at steady state. This means that the transitional phase of flow has negligible influence on the transfer. This assumption is valid for large Schmidt numbers for which the vortex relaxation time, $t_v=a^2/\nu_d$, is much shorter than the time for diffusion equilibration, $t_d=a^2/D$. To check the impact of this assumption when these time scales are comparable ($t_v=t_d$, i.e. $Sc=1$), we conducted additional simulations with a transient flow obtained by adding temporal variation of vorticity in Eqs. (4) and (6). The time history of the average Sherwood number for fixed Reynolds number $Re_d=13$ ($Re_c=197.6$) and fixed Schmidt number $Sc_d=1$ is shown on Fig. 8 for steady flow and transient flow. At the beginning, the differences between the Sherwood numbers obtained by both models are very important and the relative error can reach 80%. Gradually, as time increases, the differences between both models decline and become negligible for dimensionless times greater than about $\tau=0.001$. So the assumption of steady state flow is valid except during short start-up time. However, it is obvious that if one is interested in transfer at its initial phase, unsteady flow model is more appropriate.

6. Conclusions

Mass transfer due to the combined diffusive and convective mechanisms inside spherical bubbles moving in a stagnant liquid was modeled in this paper. Modeling is based on the Navier–Stokes and diffusion–convection equations solved numerically by the finite difference method. The results show the dependence of Sherwood number on both Red and Sc_d numbers. It is found that when $Re_d < 1$ the dependence of the rate of mass transfer on the Schmidt number is very weak. In this case, the results are quite close to the analytical solution of Newman with an error less than 3%. However, at higher values of Re_d, both the transient rate of mass transfer and its asymptotic solution depend strongly on the value of the Schmidt number. The results also show that the asymptotic values of the analytical solution of Kronig–Brink are never exceeded for spherical bubbles with Reynolds numbers $Re_d < 13$ and Schmidt numbers $Sc_d < 5$. In order to present the numerical results under a form easier to use, our numerical results are correlated by an equation. The proposed formula gives the average Sherwood number values which coincide with those calculated numerically with an error not exceeding 5% for Reynolds numbers $Re_d < 13$ and Schmidt numbers $Sc_d < 5$. Although current results provide further insight into the mass transfer within bubbles, it should be emphasized that the theoretical and computational framework developed concerns the internal regime of clean bubbles. In practice, resistance to diffusive transport may occur in both phases and the aqueous phase may contain surfactants. The main perspectives of this work would be to extend the simulations to take into account such effects.

References

Barakat, H.Z., Clark, J.A., 1966. On the solution of the diffusion equation by numerical methods. J. Heat Transf. 88, 421–427.

Chen, W.H., 2001. Dynamics of sulfur dioxide absorption in a raindrop falling at terminal velocity. Atmos. Environ. 35, 4777–4790.

Chhabra, R.P., 2006. Bubbles, Drops and Particles in Non-Newtonian Fluids. CRC Press, Boca Raton.

Clift, R., Grace, J.R., Weber, M.E., 1978. Bubbles, Drops and Particles. Academic Press, New York.

Colombet, D., Legendre, D., Cockx, A., Guiraud, P., 2013. Mass or heat transfer inside a spherical gas bubble at low to moderate Reynolds number. Int. J. Heat Mass Transf. 67, 1096–1105.

Dani, A., Cockx, A., Guiraud, P., 2006. Direct numerical simulation of mass transfer from spherical bubbles: the effect of interface contamination at low Reynolds numbers. Int. J. Chem. React. Eng. 4.

Feng, Z.G., Michaelides, E.E., 2001. Heat and mass transfer coefficients of viscous spheres. Int. J. Heat Mass Transf. 44, 4445–4454.

Hadamard, J., 1911. Mouvement permanent lent d'une sphère liquide et visqueuse dans un liquide visqueux. CRAS 152, 1735–1738.

JohnsJr., Beckmann, R.B., 1966. Mechanism of dispersed phase mass transfer in viscous, single drop extraction system. AIChE J. 12, 10–16.

Juncu, G., 1999. A numerical study of steady viscous flow past a fluid sphere. Int. J. Heat Fluid Flow 20, 414–421.

Juncu, G., 2001. Unsteady heat and/or mass transfer from a fluid sphere in creeping flow. Int. J. Heat Mass Transf. 44, 2239–2246.

Juncu, G., 2010. A numerical study of the unsteady heat/mass transfer inside a circulating sphere. Int. J. Heat Mass Transf. 53, 3006–3012.

Kronig, R., Brink, J.C., 1950. On the theory of extraction from falling droplets. Appl. Sci. Res., 142–154.

Legendre, D., Magnaudet, J., 1999. Effet de l'accélération d'un écoulement sur le transfert de masse ou de chaleur à la surface d'une bulle sphérique. C.R. Acad. Sci. Sér. IIB 327, 63–70.

Legendre, D., 2007. On the relation between the drag and the vorticity produced on a clean bubble. Phys. Fluids 19, 018102.

Lochiel, A., Calderbank, P., 1964. Mass transfer in the continuous phase around axisymmetric bodies of revolution. Chem. Eng. Sci. 19, 471–484.

Newman, A.B., 1931. The drying of porous solids: diffusion and surface emission equations. Trans. Am. Inst. Chem. Eng. 27, 203–211.

Oliver, D.L.R., Chung, J.N., 1986. Conjugate unsteady heat transfer from a spherical droplet at low Reynolds numbers. Int. J. Heat Mass Transf. 29, 879–887.

Oliver, D., De Witt, K., 1995. Heat transfer in bubbles and droplets at moderate Reynolds numbers: interior problem. Am. Inst. Chem. Eng. Symp. Ser. 306 (91), 87–92.

Rybczynski, W., 1911. Uber die fortschreitende Bewegung einer fluessigen Kugel in einem zahen Medium. Bull. Int. Acad. Sci. Crac. A, 40–46.

Saboni, A., Alexandrova, S., Karsheva, M., Gourdon, C., 2011. Mass transfer from a contaminated fluid sphere. AIChE J. 57, 1684–1692.

Saboni, A., Alexandrova, S., Mory, M., 2010. Flow around a contaminated fluid sphere. Int. J. Multiph. Flow 36, 503–512.

Saboni, A., Alexandrova, S., Spasic, A.M., Gourdon, C., 2007. Effect of the viscosity ratio on the mass transfer from a fluid sphere at low to very high Peclet numbers. Chem. Eng. Sci. 62, 4742–4750.

Sadhal, S.S., Ayyaswamy, P.S., Chung, J.N.C., 1996. Transport Phenomena With Drops and Bubbles. Springer, Berlin.

Takemura, F., Yabe, A., 1998. Gas dissolution process of spherical rising bubbles. Chem. Eng. Sci. 53, 2691–2699.

Watada, H., Hamielec, A.E., Johnson, A.I., 1970. A theoretical study of mass transfer with chemical reaction in drops. Canad. J. Chem. Eng 48, 255–261.

Zaritzky, N., Calvelo, A., 1979. Internal mass transfer coefficient within single bubbles. Theory and experiment. Can. J. Chem. Eng. 57 (1), 58–64.